Ab Initio Study of the Mechanisms of Rearrangements in $C_2B_4H_6$ and $C_2B_5H_7$

Michael L. McKee

Contribution from the Department of Chemistry, Auburn University, Auburn, Alabama 36849.
Received December 9, 1987

Abstract: A preliminary study of the rearrangement mechanisn in $C_2B_4H_6$ and $C_2B_5H_7$ was carried out with use of ab initio methods. In both carboranes a concerted parallel DSD (diamond–square–diamond) process, known as a local bond rotation, may be important. This can be visualized as the local rotation of a bonded pair of atoms about an axis which passes through the center of the bond and the center of the complex. A benzvalene-like structure 49 kcal/mol above 1,6-$C_2B_4H_6$ can undergo a local bond rotation to form 1,2-$C_2B_4H_6$. Another potential pathway to 1,2-$C_2B_4H_6$ is a different local bond rotation from a lower energy benzvalene-like structure (43 kcal/mol above 1,6-$C_2B_4H_6$) that is related to 1,2-$C_2B_4H_6$ by a DSD rearrangement. However, the latter pathway is blocked by a HOMO/LUMO crossing. In $C_2B_5H_7$, several local bond rotations are possible; the lowest energy barrier for a degenerate rearrangement is a local bond rotation forming a square capped prism as the transition state.

Carborane cage rearrangements have attracted much attention both experimentally[1-11] and theoretically.[12-20] Three general mechanisms[21] have been developed: (1) the diamond–square–diamond (DSD) mechanism,[22] (2) the triangular face rotation (Berry pseudorotation), and (3) the nonclassical–classical–nonclassical mechanism.[23] The DSD mechanism for isomerization of deltahedral structures has had much success in interpreting carborane chemistry as well as the chemistry of polyhedral cages of metal clusters. Often proposed as an alternative to the DSD mechanism, the triangular face rotation has been shown[7] not to occur in the rearrangement of $C_2B_5H_7$.

Recently, it was concluded that the DSD mechanism in $C_2B_3H_5$ and $C_2B_7H_9$ would be forbidden in the Woodward–Hoffmann sense due to a HOMO/LUMO crossing encountered along the reaction coordinate for rearrangement.[16] The fact that neither is known to rearrange is consistent with the predicted high activation barrier. In the case of $C_2B_3H_5$, other rearrangement pathways have been explored.[24] However, they were also of high energy.

The study of the mechanism of rearrangement in carboranes is complicated by the fact that the shifting connectivity required in the conversion of reactants to products does not correspond to bond breaking and bond forming as is often the case in organic reactions but rather to a shift of multi-center bonding from a three-center bond to a two-center bond plus a vacancy on boron. Large geometric changes are often accompanied by a modest change in energy. The reaction path is characterized by intermediate structures with increasing amount of "classical character" as three-center bonds are converted to more classical bonds. It is known that both polarization functions and electron correlation are important when determining the energies of structures which differ in the extent of three-center bonding,[25-28] and it would therefore be expected that both would be important when calculating the reaction path involving the conversion of a nonclassical reactant to a classical transition state or intermediate. As a preliminary step toward a theoretical description of the rearrangement mechanism, the goal of the present paper is to explore selected points on the potential energy surfaces of $C_2B_4H_6$ and $C_2B_5H_7$ as possible transition-state candidates for the rearrangement to different isomers.

Calculational Details

All calculations were carried out using the GAUSSIAN 82[29] or GAUSSIAN 86[30] program systems. Energies were determined at HF/3-21G[31] optimized geometries (Figure 1) and single-point calculations were carried out at several higher levels (Table I). Calculations at the MP2/6-31G and

(1) Onak, T.; Drake, R. P.; Dunks, G. B. *Inorg. Chem.* **1964**, *3*, 1686.
(2) Onak, T.; Fung, A. P.; Siwapinyoyos, G.; Leach, J. B. *Inorg. Chem.* **1979**, *18*, 2878–2882.
(3) Oh, B.; Onak, T. *Inorg. Chem.* **1982**, *21*, 3150–3154.
(4) Abdou, Z. J.; Abdou, G.; Onak, T.; Lee, S. *Inorg. Chem.* **1986**, *25*, 2678–2683.
(5) Ng, B.; Onak, T.; Banuelos, T.; Gomez, F.; Distefano, W. *Inorg. Chem.* **1985**, *24*, 4091–4096.
(6) Ng, B.; Onak, T.; Fuller, K. *Inorg. Chem.* **1985**, *24*, 4371–4376.
(7) Abdou, Z. J.; Soltis, M.; Oh, B.; Siwap, G.; Banuelos, T.; Nam, W. Onak, T. *Inorg. Chem.* **1985**, *24*, 2363–2367.
(8) Nam, W.; Onak, T. *Inorg. Chem.* **1987**, *26*, 48–52.
(9) Takimoto, C.; Siwapinyoyos, G.; Fuller, K.; Fung, A. P.; Liauw, L.; Jarvis, W.; Millhauser, G.; Onak, T. *Inorg. Chem.* **1980**, *19*, 107–110.
(10) Odom, J. D. In *Comprehensive Organometallic Chemistry*; Pergamon: Oxford, England, 1982; Vol. 1, pp 411–457.
(11) Fehlner, T. P.; Housecroft, C. E. In *Molecular Structures and Energetics*; Liebman, J. F., Greenberg, A., Eds.; Verlag Chemie International: Deerfield Beach, FL, 1984; Vol 1.
(12) Gimarc, B. M.; Ott, J. J. In *Graph Theory and Topology in Chemistry*; King, R. B., Rouvrag, D. H., Eds.; Elsevier: New York, 1987; pp 285–301.
(13) Ott, J. J.; Gimarc, B. M. *J. Comput. Chem.* **1986**, *7*, 673–692.
(14) Gimarc, B. M.; Ott, J. J. *J. Am. Chem. Soc.* **1987**, *109*, 1388–1392.
(15) Gimarc, B. M.; Ott, J. J. *Inorg. Chem.* **1986**, *25*, 2708–2711.
(16) Gimarc, B. M.; Ott, J. J. *Inorg. Chem.* **1986**, *25*, 83–85.
(17) King, R. B.; Rouvray, D. H. *J. Am. Chem. Soc.* **1977**, *99*, 7834–7840.
(18) King, R. B. *Inorg. Chim. Acta* **1981**, *49*, 237–240.
(19) King, R. B. *Theor. Chim. Acta* **1984**, *64*, 439. King, R. B. *Inorg. Chem.* **1985**, *24*, 1716.
(20) Wales, D. J.; Stone, A. J. *Inorg. Chem.* **1987**, *26*, 3845–3850.
(21) Recently a new mechanism has been proposed for rearrangement in polyhedra called the single edge cleavage process (SEC). The rearrangement can be viewed as a capped–bridged–capped rearrangement. Johnson, B. F. C. *J. Chem. Soc., Chem. Commun.* **1986**, 27–30.
(22) Lipscomb, W. N. *Science* **1966**, *153*, 373–378.
(23) Camp, R. N.; Marynick, D. S.; Graham, G. D.; Lipscomb, W. N. *J. Am. Chem. Soc.* **1978**, *100*, 6781–6783.
(24) McKee, M. L. *THEOCHEM*, in press.
(25) McKee, M. L.; Lipscomb, W. N. *Inorg. Chem.* **1981**, *20*, 4452.
(26) McKee, M. L.; Lipscomb, W. N. *Inorg. Chem.* **1981**, *20*, 4442.
(27) McKee, M. L.; Lipscomb, W. N. *Inorg. Chem.* **1982**, *21*, 2846.
(28) McKee, M. L.; Lipscomb, W. N. *Inorg. Chem.* **1985**, *24*, 765.
(29) Binkley, J. S.; Frisch, M.; Raghavachari, K.; Fluder, E.; Seeger, R.; Pople, J. A. GAUSSIAN 82; Carnegie-Mellon University.
(30) GAUSSIAN 86, Frisch, M. et al., Carnegie-Mellon Quantum Chemistry Publishing Unit, Carnegie-Mellon University, Pittsburgh, PA 15213.
(31) References to basis sets and methods used are collected here. 3-21G basis: Binkley, J. S.; Pople, J. A.; Hehre, W. J. *J. Am. Chem. Soc.* **1980**, *102*, 939. 6-31G basis: Hehre, W. J.; Ditchfield, R.; Pople, J. A. *J. Chem. Phys.* **1972**, *56*, 2257. 6-31G* basis: Hariharan, P. C.; Pople, J. A. *Theor. Chim. Acta* **1973**, *28*, 213. Gordon, M. S. *Chem. Phys. Lett.* **1980**, *76*, 163. Francl, M. M.; Pietro, W. J.; Hehre, W. J.; Binkley, J. S.; Gordon, M. S.; Defrees, D. J.; Pople, J. A. *J. Chem. Phys.* **1977**, *77*, 3654. MP2 correlation treatment: Møller, C.; Plesset, M. S. *Phys. Rev.* **1934**, *46*, 618. Pople, J. A.; Binkley, J. S.; Seeger, R. *Int. J. Quantum Chem. Symp.* **1976**, *10*, 1. CPHF: Pople, J. A.; Krishnan, R.; Schlegel, H. B.; Binkley, J. S. *Int. J. Quantum Chem. Sym.* **1979**, *13*, 225.

0002-7863/88/1510-5317$01.50/0

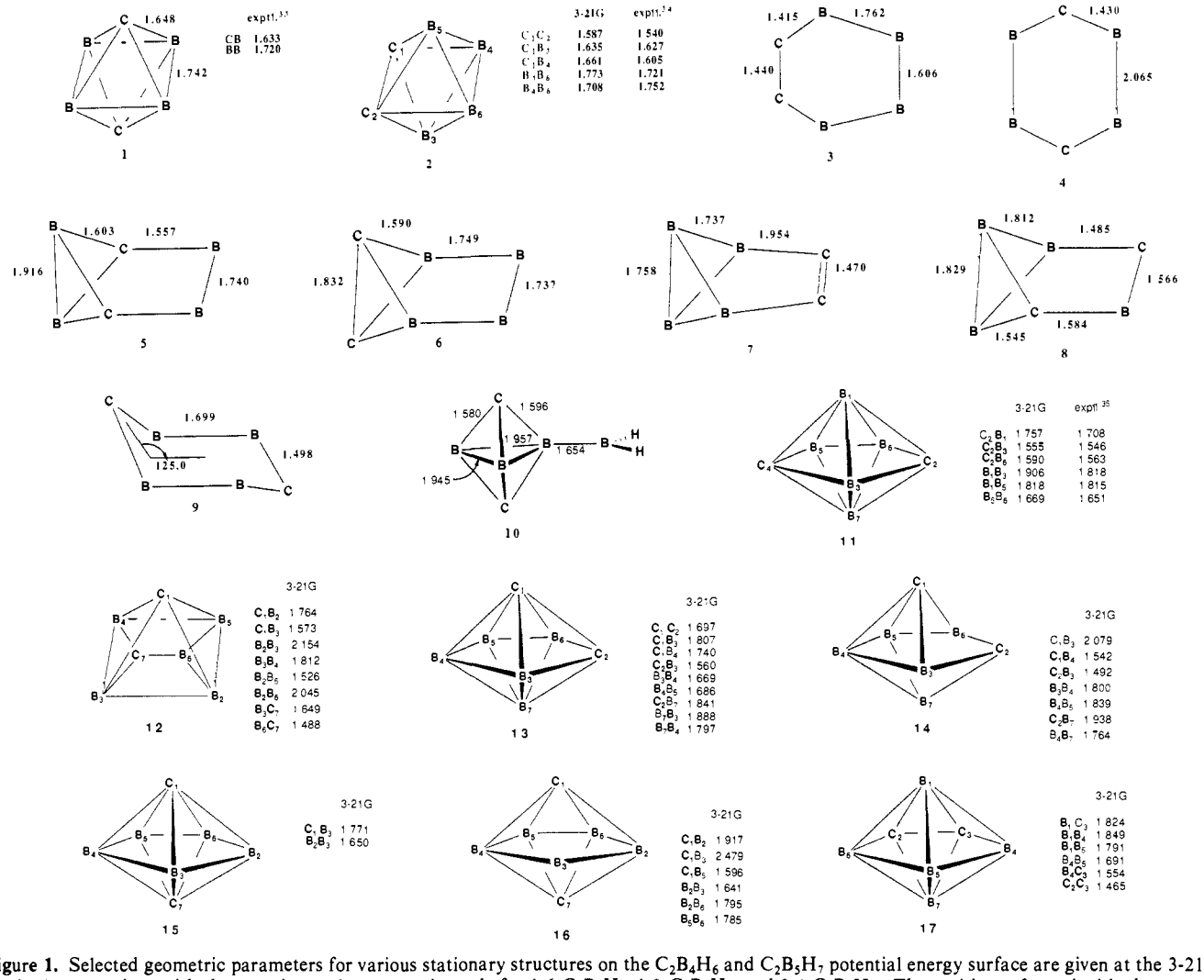

Figure 1. Selected geometric parameters for various stationary structures on the $C_2B_4H_6$ and $C_2B_5H_7$ potential energy surface are given at the 3-21G level. A comparison with the experimental structure is made for 1,6-$C_2B_4H_6$, 1,2-$C_2B_4H_6$, and 2,4-$C_2B_5H_7$. The positions of terminal hydrogens on carbon and boron have been fully optimized but are not included in the figure for clarity.

Table I. Total Energies (hartrees) and Zero-Point Energies (kcal/mol) of Species on the $C_2B_4H_6$ (**1–10**) and $C_2B_5H_7$ (**11–17**) Potential Energy Surfaces

		sym	3-21G	6-31G	MP2/6-31G[a]	6-31G*	MP2/6-31G*[a]	ZPE(NEV)[b]
1	1,6-$C_2B_4H_6$	D_{4h}	−176.917 62	−177.838 64	−178.263 82	−177.943 16	−178.558 96	56.88 (0)
2	1,2-$C_2B_4H_6$	C_{2v}	−176.909 65	−177.828 60	−178.248 38	−177.932 70	−178.542 98	57.08 (0)
3	1,2-planar	C_{2v}	−176.613 01	−177.542 58	−177.969 79	−177.611 43		52.22 (4)
4	1,4-planar	C_{2v}	−176.729 85	−177.657 06	−178.108 60	−177.707 16		47.74 (3)
5	benzvalene-like	C_{2v}	−176.928 98	−177.853 15	−178.233 94	−177.928 05	−178.489 51	55.96 (0)
6	benzvalene-like	C_{2v}	−176.729 82	−177.655 07	−178.053 92	−177.726 07		51.90 (2)
7	benzvalene-like	C_{2v}	−176.826 64	−177.751 43	−178.171 19	−177.831 16	−178.433 43	54.07 (2)
8	benzvalene-like	C_s	−176.896 57	−177.819 15	−178.220 34	−177.896 09	−178.477 98	55.34 (1)
9	chair hexane-like	C_{2h}	−176.857 67	−177.787 20	−178.188 25	−177.843 81	−178.415 26	53.11 (1)
10	*exo*-BH_2	C_{2v}	−176.924 36	−177.848 70	−178.230 75	−177.930 16	−178.494 13	55.56 (0)
11	2.4-$C_2B_5H_7$	C_{2v}	−202.082 10	−203.133 65	−203.614 25	−203.242 05		67.26 (0)
12	square-capped prism	C_s	−201.993 11	−203.047 18	−203.525 02	−203.143 04		64.04 (1)
13	1,2-$C_2B_5H_7$	C_{2v}	−202.011 15	−203.059 22	−203.547 38	−203.166 77		66.16 (0)
14	1,2-$C_2B_5H_9$ (open)	C_s	−202.007 06	−203.059 28	−203.547 15	−203.155 90		64.92 (0)
15	1,7-$C_2B_5H_7$	D_{5h}	−201.958 05	−203.006 20	−203.506 19	−203.112 84		65.41 (0)
16	1,7-$C_2B_5H_7$ (open)	C_{2v}	−201.951 01	−203.002 20	−203.482 80	−203.103 52		64.79 (0)
17	2,3-$C_2B_5H_7$	C_{2v}	−202.051 10	−203.101 99	−203.587 50	−203.211 29		66.87 (0)

[a] MP2 calculations are made with the frozen core approximation. [b] Zero-point energies in kcal/mol are given with the number of negative eigenvalues (NEV) given in parentheses.

HF/6-31G* levels were used to approximate relative energies at the MP2/6-31G* level with use of the additivity approximation[32] (Table II). In order to determine the success of this approximation the full MP2/6-31G* calculations were made on some 3-21G stationary points. Stationary points were characterized by calculating vibrational frequencies. Selected geometric parameters for the structures **1–17** and a comparison with the experimental structures for 1,6-$C_2B_4H_6$,[33] 1,2-$C_2B_4H_6$,[34] and 2,4-$C_2B_5H_7$[35] are given in Figure 1. The calculated geometries of 1,6-

(32) (a) McKee, M. L.; Lipscomb, W. N. *J. Am. Chem. Soc.* **1981**, *103*, 4673. (b) Nobes, R. H.; Bouma, W. J.; Radom, L. *Chem. Phys. Lett.* **1982**, *89*, 497. (c) McKee, M. L.; Liscomb, W. N. *Inorg. Chem.* **1985**, *24*, 762.

(33) McNeill, E. A.; Gallaher, K. L.; Scholer, F. R.; Bauer, S. H. *Inorg. Chem.* **1973**, *12*, 2108.

(34) Beaudet, R. A.; Poynter, R. L. *J. Chem. Phys.* **1970**, *53*, 1899.

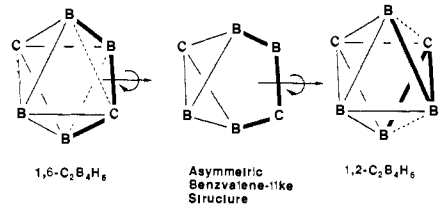

Figure 2. A rotation by 90° about the BH–CH bond in 1,6-$C_2B_4H_6$ will yield the benzvalene-like structure and continued rotation by 90° will yield 1,2-$C_2B_4H_6$.

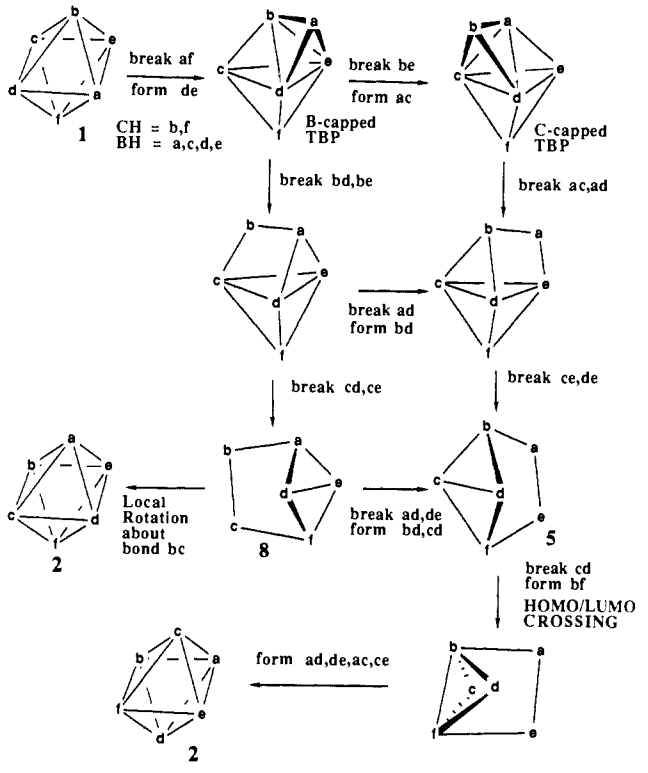

Figure 3. A reaction scheme is presented for the conversion of 1,6-$C_2B_4H_6$ (top) to 1,2-$C_2B_4H_6$ (bottom). The 1,6-$C_2B_4H_6$ isomer can form the benzvalene-like structures **5** by a local bond rotation about the "ae" bond. Formation of the 1,2-$C_2B_4H_6$ isomer from **5** is blocked by a HOMO/LUMO crossing. On the other hand **8** can form the 1,2-$C_2B_4H_6$ isomer by another local bond rotation.

$C_2B_4H_6$, 1,2-$C_2B_4H_6$, and 2,4-$C_2B_5H_7$ have been reported at the HF/STO-3G[13,36] and HF/3-21G[37] levels.

$C_2B_4H_6$ Rearrangement. It is known that the 1,2-$C_2B_4H_6$ isomer rearranges to the more stable, 1,6-$C_2B_4H_6$ isomer at a temperature of about 250–300 °C.[9] Several theoretical studies have attempted to clarify the mechanism of rearrangement.[38,39] A PRDDO study,[39] which used a linear (and quadratic) synchronous transit, reported a "sagging sawhorse" as an intermediate separated by barriers of 27 and 14 kcal/mol from 1,2-$C_2B_4H_6$ and 1,6-$C_2B_4H_6$, respectively. A later PRDDO study[23] reported a revised structure of the intermediate which resembled the benzvalene structure of C_6H_6. At the PRDDO level[40] the intermediate was predicted to be 31 kcal/mol more stable than 1,2-$C_2B_4H_6$ and 20 kcal/mol more stable than 1,6-$C_2B_4H_6$. Since the benzvalene form has not been observed, the stability of the intermediate must have been overestimated.

Ten structures were optimized on the $C_2B_4H_6$ potential energy surface (Figure 1) including the two known structures, 1,6-$C_2B_4H_6$ (**1**) and 1,2-$C_2B_4H_6$ (**2**). The remaining eight have not been observed but may play a role in the gas-phase interconversion of 1,2-$C_2B_4H_6$ to 1,6-$C_2B_4H_6$. The two planar structures that were considered (**3** and **4**) were both stationary points of higher order (>2 negative eigenvalues of force constant matrix). Since they are much higher in energy than **1** or **2**, neither can be important in the rearrangement. Structures **5**–**8** are benzvalene-like structures that differ in the placement of the two carbons. Attempts to optimize a benzavalene-like structure of C_1 symmetry with one carbon in the "jaws" and one in the trivalent position resulted in a species similar to **9** which has C_{2h} symmetry. The transformation from the asymmetric benzvalene-like structure to 9, which is shown in Figure 2, involves the breaking of opposite bonds and is analogous to the ring opening of bicyclobutane to butadiene. Structure **10**, a BH_2-substituted trigonal bipyramid, is included for comparison. However, since the interconversion does not scramble terminal sites, **10** cannot be on the reaction pathway.

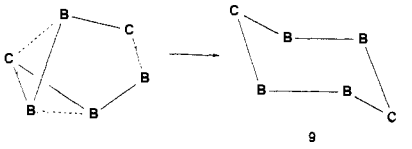

Figure 4. Indication of the geometric change which occurs when the indicated asymmetric benzvalene-like structure is optimized in C_1 symmetry. The C_{2h} symmetry structure is still characterized by a small negative eigenvalue of the force constant matrix which indicates that a distort from C_{2h} symmetry is favorable at the HF/3-21G level.

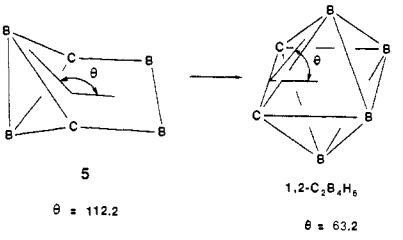

Figure 5. Definition of the parameter that was varied in the construction of the reaction path connecting the benzvalene-like structure **5** (on left) and 1,2-$C_2B_4H_6$ (on right).

A capped trigonal bipyramid was considered (Figure 3) since such a species would be the transition state in a *closo* → *hypo-closo* → *closo* mechanism.[41] It has been pointed out[42] that capped structures are generally unfavorable due to the fact that the s and p valence orbitals of boron do not provide sufficient overlap above a triangular face. In fact in the course of geometry optimization the capped trigonal bipyramid collapsed to the unsymmetrically substituted benzvalene-like structure (**8**).

Several alternative pathways are presented in Figure 3 for the conversion of 1,6-$C_2B_4H_6$ to 1,2-$C_2B_4H_6$. A boron-capped or carbon-capped trigonal bipyramid can be formed which can relax to form an intermediate "bridged trigonal bipyramid" by lengthening two of the interactions of the apex with the equatorial borons or further relax to a more classical benzvalene-like structure **5** or **8**. Alternatively, **5** can be formed from **1** directly by a local bond rotation about the "ae" bond in **1** (Figure 3). Local bond rotation is a term used for a concerted parallel DSD process that can be visualized as the local bond rotation of a bonded pair of atoms about an axis that passes through the center of the bond and the center of the complex.

Two other benzvalene-like structures can be formed by local bond rotations in **1** or **2**, forming **6** and **7** which differ in the location of the two carbon atoms. In **6** the two carbon atoms are located in the benzvalene "jaws" while in **7** the two carbon atoms are adjacent and form a relatively short interaction (1.47 Å). Both structures are too high in energy relative to **1** or **2** (Table II) to be considered in the rearrangement. The asymmetric benzvalene-like structure in Figure 4 is the only structure that can be related to both 1,6-$C_2B_4H_6$ and 1,2-$C_2B_4H_6$ by local bond rotations. This structure could not be located due to its low symmetry (C_1); however, its energy might be expected to be intermediate to structure **6** in which both carbons are located in the "jaws" and **7** in which both carbons are located in the trivalent positions which would be about 109 kcal/mol above 1,6-$C_2B_4H_6$ at the [MP2/6-31G*] + ZPC level ((147.9 + 70.9)/2, Table II). Structure **9**, which is derived from the collapse of the asymmetric benzvalene-like structure (Figure 2), is 86.4

(35) Beaudet, R. A.; Poynter, R. L. *J. Chem. Phys.* **1965**, *43*, 2166.
(36) The 1,6-$C_2B_4H_6$ and 1,2-$C_2B_4H_6$ geometries are reported. Whelan, T.; Brint, P. *J. Chem. Soc. Faraday Trans. 2* **1985**, *81*, 267–276.
(37) The 1,6-$C_2B_4H_6$ and 2,4-$C_2B_5H_7$ geometries are reported. McKee, M. L., submitted.
(38) Cheung, C. C. S.; Beaudet, R. A.; Segal, G. A. *J. Am. Chem. Soc.* **1970**, *92*, 4158.
(39) Halgren, T. A.; Pepperberg, I. M.; Lipscomb, W. N. *J. Am. Chem. Soc.* **1975**, *97*, 1248–1250.
(40) Halgren, T. A.; Kleier, D. A.; Hall, J. H.; Brown, L. D.; Lipscomb, W. N. *J. Am. Chem. Soc.* **1978**, *100*, 6595–6608.
(41) Johnston, R. L.; Mingos, D. M. P. *Inorg. Chem.* **1986**, *25*, 3321–3323.
(42) Jemmis, E. D. *J. Am. Chem. Soc.* **1982**, *104*, 7017.

Table II. Energies (kcal/mol) of Species Relative to 1,6-$C_2B_4H_6$ (**1**–**10**) and 2,4-$C_2B_5H_7$ (**11**–**17**)

		3-21G	6-31G	MP2/6-31G	6-31G*	[MP2/6-31G*] (+ZPC)[a,b]	MP2/6-31G* (+ZPC)[b]
1	1,6-$C_2B_4H_6$	0.0	0.0	0.0	0.0	0.0 (0.0)	0.0 (0.0)
2	1,2-$C_2B_4H_6$	5.0	6.3	9.7	6.6	10.0 (10.2)	10.0 (10.2)
3	1,2-planar	191.2	185.8	184.6	208.2	207.0 (202.3)	
4	1,4-planar	117.9	114.0	97.4	148.1	131.5 (122.4)	
5	benzvalene-like	−7.1	−9.1	18.8	9.5	37.4 (36.5)	43.6 (42.7)
6	benzvalene-like	117.9	115.2	131.8	136.3	152.9 (147.9)	
7	benzvalene-like	57.1	54.7	58.1	70.3	73.7 (70.9)	78.8 (76.0)
8	benzvalene-like	13.2	12.2	27.3	29.5	44.6 (43.1)	50.8 (49.3)
9	chair hexane-like	37.6	32.3	47.4	62.4	77.5 (73.7)	90.2 (86.4)
10	*exo*-BH_2	−4.2	−6.3	20.8	8.2	35.3 (34.0)	40.7 (39.4)
11	2,4-$C_2B_5H_7$	0.0	0.0	0.0	0.0	0.0 (0.0)	
12	square-capped prism	55.8	54.3	56.0	62.1	63.8 (60.6)	
13	1,2-$C_2B_5H_7$	44.5	46.7	42.0	47.2	42.5 (41.4)	
14	1,2-$C_2B_5H_7$ (open)	47.1	46.7	42.1	54.1	49.5 (47.2)	
15	1,7-$C_2B_5H_7$	77.9	80.0	67.8	81.1	68.9 (67.1)	
16	1,7-$C_2B_5H_7$ (open)	82.3	82.5	82.5	87.0	87.0 (84.5)	
17	2,3-$C_2B_5H_7$	19.4	19.9	16.8	19.3	16.2 (15.8)	

[a] Relative energies are computed with use of the additivity approximation[32] while zero-point corrected relative energies are given in parentheses. [b] Zero-point corrections are made from frequency calculations at the HF/3-21G level.

Table III. Reaction Path Constructed from **5** to 1,2-$C_2B_4H_6$[a]

reaction coordinate[b]	6-31G	MP2/6-31G	6-31G*	[MP2/6-31G*]
112.2	−20.0	6.6	−5.5	21.1
90.0	16.4	32.3	26.0	41.9
85.0	28.8	38.9	36.4	46.5
80.0	40.8	45.8	46.6	51.6
75.0	53.6	55.1	57.9	59.4
85.0	65.9	62.4	75.0	71.5
80.0	45.0	43.5	52.5	51.0
75.0	26.9	26.5	32.5	32.1
63.2	0.0	0.0	0.0	0.0

[a] Geometries were optimized at the MNDO level, and single-point calculations were made at the MP2/6-31G and HF/6-31G* levels in order to estimate relative energies at the MP2/6-31G* level. [b] For a description of the reaction coordinate see Figure 5.

kcal/mol above 1,6-$C_2B_4H_6$ and is also too high in energy to be considered as a transition state.

On the other hand, **5** is 42.7 kcal/mol higher than **1** and **8** is 49.3 kcal/mol higher. If **5** or **8** were the transition state for rearrangement, the barrier height would be the energy relative to **2** (1,2-$C_2B_4H_6$), since the observed rearrangement is in the direction **2** → **1**. With respect to **2**, **5** and **8** are 32.5 and 39.1 kcal/mol higher in energy, respectively.

From the benzvalene structure **5**, the lowest energy benzvalene-like structure, a DSD mechanism can be envisioned (Figure 3) that would give a structure with adjacent carbons. Folding back the "jaws" then yields the 1,2-$C_2B_4H_6$ isomer. However, the interconversion is blocked by a HOMO/LUMO crossing that is encountered along the reaction path. In order to obtain a qualitative understanding of the crossing, a MNDO reaction cut was constructed from **5** and from **1** by using a chosen value of θ (Figure 5) and optimizing all other parameters (within C_{2v} symmetry) at the MNDO level. The resulting geometries were then used for single-point calculations at the MP2/6-31G and HF/6-31G* levels in order to estimate relative energies at the MP2/6-31G* level (Table III, Figure 6). The two curves in Figure 6 represent different orbital occupancies. Points on the left-hand side have four b_1 orbitals occupied and five b_2 orbitals occupied which is the same occupation as the benzvalene structure **5**, while on the right-hand side the $3b_1$:$6b_2$ occupation corresponds to the orbital occupation of 1,2-$C_2B_4H_6$. Each curve represents the optimized geometry at a particular value of θ and for either the $4b_1$:$5b_2$ or $3b_1$:$6b_2$ orbital occupation; hence the crossing of the two curves does not occur at the same geometry. The energy difference between 1,2-$C_2B_4H_6$ and the benzavalene-like **5** is underestimated when the MNDO geometries[43] are used (20.1 kcal/mol) as compared to 3-21G geometries (37.4 kcal/mol) when relative energies are evaluated by using the additivity approximation. However, the crossing point is located about 30 kcal/mol above **5** in Figure 6 and the barrier is likely to remain significant when more sophisticated methods are used. Therefore rearrangment of **5** to 1,2-$C_2B_4H_6$ is not likely to occur by a DSD mechanism.

(43) Dewar, M. J. S.; McKee, M. L. *J. Am. Chem. Soc.* **1977**, *99*, 5231.

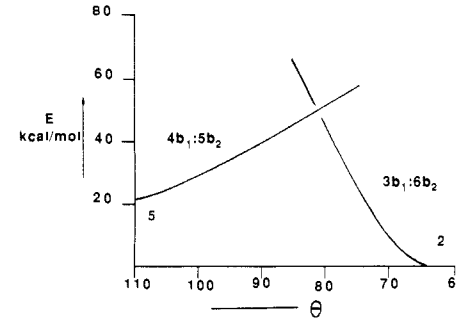

Figure 6. Reaction profile obtained when θ is varied from the optimized value in the benzvalene-like structure (112.2°) to the optimized value in 1,2-$C_2B_4H_6$ (63.2°). The curve on the left has a configuration of four b_1 and five b_2 orbitals occupied ($4b_1$:$5b_2$) while the curve on the right has a configuration of three b_1 and six b_2 orbitals occupied ($3b_1$:$6b_2$). The graph is constructed from the values in Table III. At each MNDO optimized geometry (with θ constrained) single-point calculations at the MP2/6-31G and HF/6-31G* levels were carried out in order to estimate relative energies at the MP2/6-31G* level.

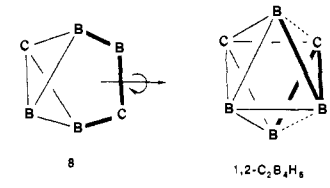

Figure 7. A local bond rotation in **8** will yield 1,2-$C_2B_4H_6$ (**2**).

A similar HOMO/LUMO crossing was encountered[24] in the DSD rearrangement of 1,2-$C_2B_3H_5$ to 1,5-$C_2B_3H_5$. The limitations to the description of the crossing which were stated in that study apply to the present situation as well.

While the reaction path **5** to **2** is blocked by a HOMO/LUMO crossing, a local bond rotation will take **8** to **2**. An illustration of the required local rotation is shown in Figure 7. The atoms involved in the local bond rotation are shown connected by heavy lines where the two end atoms can be visualized as fixed during the rotation of the other two atoms. If **8** is the highest point on that reaction path, the calculated barrier would be 39.1 kcal/mol with respect to 1,2-$C_2B_4H_6$. From an estimation of the reaction time and temperature Lipscomb and coworkers[39] have estimated the barrier to be 42–45 kcal/mol.

A weakness of the present analysis is that computational evidence is not presented that the reaction pathway necessary to convert 1,6-$C_2B_4H_6$ to **8** may not encounter a higher energy structure (Figure 3). The most likely pathway is a local bond rotation to convert 1,6-$C_2B_4H_6$ to the benzvalene-like structure **5** which may then be converted to **8** by breaking and forming two bonds (Figure 3).

One interesting prediction is that while **5** will not lead to the 1,2-$C_2B_4H_6$ isomer, it would be the transition state for degenerate rearrangement of terminal boron substituents. Hence, the 2,3-Me_2-1,6-

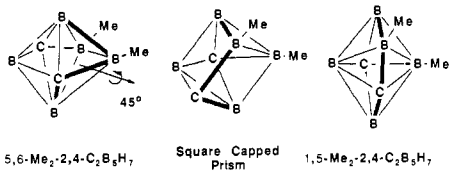

Figure 8. A local bond rotation in $5,6\text{-}Me_2\text{-}2,4\text{-}C_2B_5H_5$ about the indicated axis by 45° will yield the square-capped prism. A further rotation about the same axis by 45° will yield $1,5\text{-}Me_2\text{-}2,4\text{-}C_2B_5H_5$.

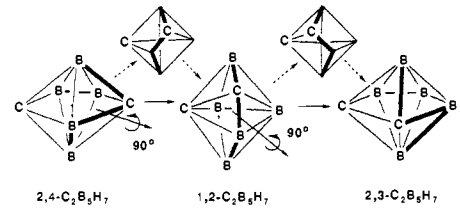

Figure 9. A local bond rotation about the indicated axis by 90° will yield first the $1,2\text{-}C_2B_5H_7$ isomer and then the $2,3\text{-}C_2B_5H_7$ isomer. Taken in the opposite direction the pathway describes the conversion of the 2,3-isomer to the 2,4-isomer which is observed to take place at 320 °C. Rotation by 45° gives the square-capped prisms (shown inbetween the 2,4- and 1,2-isomers and inbetween the 1,2- and 2,3-isomers) which are the likely transition states in the interconversion.

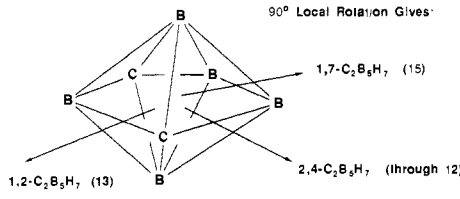

Figure 10. Rotations about the indicated axes in $2,4\text{-}C_2B_5H_7$ will yield the 1,2-, 2,4-, or $1,7\text{-}C_2B_5H_7$ isomers. In each case, the rotated bonded pair in $2,4\text{-}C_2B_5H_7$ (i.e., BH–BH or BH–CH) becomes two of the equatorial vertices in the pentagonal bipyramidal structure.

$C_2B_4H_4$ isomer is predicted to be in equilibrium with the $2,4\text{-}Me_2\text{-}1,6\text{-}C_2B_4H_4$ isomer with a kinetic barrier of 42.7 kcal/mol.

$C_2B_5H_7$ Rearrangement. It is known[2] that at a temperature of 300 °C an equilibrium can be established among the different isomers of mono-B-methylated $C_2B_5H_7$. In addition it is known that $5,6\text{-}Me_2\text{-}2,4\text{-}C_2B_5H_5$ preferrentially forms the 1,5-dimethyl isomer prior to the 1,3-, 3,5-, and 1,7-isomers.[5] This fact is taken as evidence for a local bond rotation ("edge-twist")[3] that would yield the 1,5-isomer as indicated in Figure 8. A local bond rotation of about 45° gives a square-capped prism that may be a transition state or intermediate in the degenerate rearrangement. As indicated in Figures 9 and 10 local bond rotations about the adjacent CB bond and the BB bond yield $1,2\text{-}C_2B_5H_7$ and $1,7\text{-}C_2B_5H_7$. In both cases local rotation of 45° will give a square-capped prism that may be a transition state, intermediate, or simply a point on the reaction surface, while the 90° local bond rotation will be either a transition state or intermediate.

Six structures on the $C_2B_5H_7$ potential energy surface were optimized at the HF/3-21G level. The known isomer $2,4\text{-}C_2B_5H_7$ and the 1,2- and 1,7-pentagonal bipyramids were optimized within their respective point groups (Figure 1). There is good agreement between theory and experiment on the structure of $2,4\text{-}C_2B_5H_7$. What is perhaps surprising is the good agreement between low-level calculations (STO-3G) and the much better calculations presented here for the relative energies of the three isomers. At the STO-3G level[13] the 1,2-, 1,7-, and 2,3-isomers are 49.8, 79.8, and 24.2 kcal/mol less stable than the $2,4\text{-}C_2B_5H_7$ isomer, while at the [MP2/6-31G*] plus zero-point correction level the differences are 41.4, 67.1, and 15.8 kcal/mol, respectively. The $C_2B_5H_7$ potential energy surface, in contrast to the $C_2B_4H_6$ potential energy surface, does not seem to be sensitive to electron correlation or polarization functions as indicated by the fact that the ordering of species at the HF/6-31G level is preserved at the MP2/6-31G and HF/6-31G* levels. These results may indicate that results of lower level calculations may be qualitatively correct when studying rearrangement mechanisms in the larger carboranes.

Two classical structures were discovered on the $C_2B_5H_7$ potential energy surface that are related to the pentagonal bipyramid structures but more open. Structure **14**, which is related to $1,2\text{-}C_2B_5H_7$ (**13**), has very short CB distances between C_2B_3/C_2B_6 (1.492 Å) and C_1B_4/C_1B_5 (1.542 Å) and much longer distances between C_1C_2, C_1B_3, C_1B_6, B_3B_7, and B_6B_7. Despite the large geometric differences between **14** and $1,2\text{-}C_2B_5H_7$ (**13**), the energies are very similar. The strengthening of two-center interactions comes at the expense of weakening other three-center interactions. At the highest level **14** is only 5.8 kcal/mol less stable than the $1,2\text{-}C_2B_5H_7$ isomer. While a barrier must exist at the HF/3-21G level since both are predicted to be mimina, it is not known whether a barrier would also exist at higher levels of calculation.

A more classical structure (**16**) also exists near the $1,7\text{-}C_2B_5H_7$ isomer (**15**). The apical carbon atoms have shifted from the fivefold axis (Figure 1) and increased the distance to one equatorial boron (1.771 Å → 2.479 Å) and decreased the distances to the two opposite borons (1.771 Å → 1.596 Å). At the HF/3-21G level **16** is only 4.4 kcal/mol less stable than the more symmetrical **15**. However, correlation definitely favors **15** over **16**, and at the highest level **15** is 17.4 kcal/mol more stable than **16**. Both structures are calculated to be stable minima at the HF/3-21G level.

The mechanism with the lowest energy barrier which can explain the sequence of dimethyl isomers formed from the 5,6-dimethyl isomer is a local bond rotation about the B–C bond in the $2,4\text{-}C_2B_5H_7$ isomer (Figure 8).[12] The square-capped prism, which is formed after about a 45° rotation, is predicted to be the transition state at the HF/3-21G level and at the [MP2/6-31G*] plus zero-point correction level leads to a predicted barrier of 60.6 kcal/mol. This value is certainly too large since a reaction temperature of about 300 °C would suggest a barrier in the 35 to 45 kcal/mol range. However, a more accurate determination of the transition-state geometry and additional electron correlation may bring this value down. Also, it should be noted that the observed reaction is for the dimethyl-substituted carborane which may rearrange more readily.

The recently observed rearrangement[44] of $2,3\text{-}Et_2\text{-}C_2B_5H_5$ to $2,4\text{-}Et_2\text{-}C_2B_5H_5$ which occurs at 320 °C can be interpreted by a slightly different mechanism (Figure 9). The reaction would proceed over one square capped prism transition state to form the $1,2\text{-}C_2B_5H_7$ isomer, which is 41.4 kcal/mol less stable than the $2,4\text{-}C_2B_5H_7$ isomer, and finally over the second square capped transition state to form the $2,4\text{-}C_2B_5H_7$ isomer. The fact that the $1,2\text{-}C_2B_5H_7$ isomer is not observed must indicate that one of the square capped prism transition states which lead to the $1,2\text{-}C_2B_5H_7$ isomer must be too low to give kinetic stability.

Conclusion

The $1,2\text{-}C_2B_4H_6$ and $2,4\text{-}C_2B_5H_7$ carboranes are predicted to rearrange by a concerted parallel DSD mechanism that we call "local bond rotation". On the basis of an assumed transition state (**8**), the $1,2\text{-}C_2B_4H_6$ isomer has a predicted barrier to formation of the more stable $1,6\text{-}C_2B_4H_6$ isomer of about 39.1 kcal/mol, which is in good agreement with an experimental estimate of 42–45 kcal/mol. The predicted barrier in the degenerate rearrangement of $2,4\text{-}C_2B_5H_7$ is too high (60.6 kcal/mol) since a reaction temperature of about 300 °C would imply a smaller barrier (35–45 kcal/mol).

Acknowledgment. We thank the donors of the Petroleum Research Fund, administered by the American Chemical Society, for financial support and Drs. U. Peter and T. Webb for a careful reading of the manuscript. Computer time for this study was donated by the Auburn University Computer Center.

Registry No. 1, 20693-67-8; **2**, 20693-68-9; **3**, 68691-58-7; **4**, 115093-21-5; **5**, 68732-09-2; **10**, 114467-67-3; **11**, 20693-69-0; **12**, 115093-22-6; **13**, 25036-76-4; **15**, 25036-79-7; **17**, 30347-95-6.

(44) Beck, J. S.; Kahn, A. P.; Sneddon, L. G. *Organometallics* **1986**, *5*, 2552–2553.